Synchrotron SAXS and Laser Light Scattering Studies of Aggregation Behavior of Poly(1,1-dihydroperfluorooctyl acrylate-*b*-vinyl acetate) Diblock Copolymer in Supercritical Carbon Dioxide

Li-Zhi Liu, Zhigang Cheng, Katsuhiro Inomata, Shuiqin Zhou, and Benjamin Chu*

Department of Chemistry, State University of New York at Stony Brook, Stony Brook, Long Island, New York 11794-3400

Received June 16, 1998; Revised Manuscript Received July 16, 1999

ABSTRACT: The aggregation behavior of dilute poly(1,1-dihydroperfluorooctyl acrylate-*b*-vinyl acetate) diblock copolymer in supercritical carbon dioxide ($SCCO_2$) has been studied by using synchrotron small-angle X-ray scattering (SAXS) for the following two processes: an isothermal process with changes in pressure and a cooling process at a constant pressure. The above two processes also made it possible to compare the phase behavior of the solution at a constant $SCCO_2$ density. The SAXS study, together with some light scattering experiments, shows that the phase behavior of the copolymer changes dramatically with experimental conditions in the $SCCO_2$ solvent. The soluble solution was obtained at a low pressure of 180 bar with a corresponding $SCCO_2$ density $\rho \sim 0.65$ g/cm^3 and at a high pressure at 450 bar with $\rho \sim 0.90$ g/cm^3 for the isothermal process at 65 °C. In the isothermal process, large aggregates exhibiting domain-packing structures were formed in the pressure range from 190 to 226 bar. Block copolymer micelles were observed at 243 bar and 65 °C, and the micellar behavior of the solution was then studied either by increasing the pressure at a constant temperature (65 °C) or by decreasing the temperature at a constant pressure (243 bar). The micellar size shows a similar dependence on the solution density for the above two processes. However, at a given $SCCO_2$ density, the phase behavior of the solution could be very different, including the species present and the micellar size, suggesting that the copolymer solution behavior in $SCCO_2$ cannot be simplified only in terms of the $SCCO_2$ density dependence, even though density is a crucial parameter which is intimately related to the solvent quality of $SCCO_2$.

Introduction

In the supercritical fluid (SCF) region, where the fluid temperature and pressure are above those of the critical point, the properties of the fluid are uniquely different from those of a normal gas or liquid but are often intermediate between them.[1,2] Diffusion coefficients are 10−100 times higher in SCFs than in the correponding liquid state, which is a significant advantage for applications that depend on transport processes. SCFs are also becoming increasingly important solvent systems for use in polymer science and engineering.[3] Supercritical CO_2 ($SCCO_2$), in particular, is widely used as a solvent due to its low cost, moderate critical conditions (T_c = 31.1 °C, P_c = 73.8 bar), and environmentally benign nature, making it a good replacement for some toxic organic solvents. $SCCO_2$ has been used successfully in emulsion polymerization, as most polymers are not soluble in $SCCO_2$ and cannot be synthesized in $SCCO_2$ by the homogeneous polymerization method. Diblock copolymers with a "CO_2-philic" block have been shown to be a very effective surfactant for emulsion polymerization.[4,5] Therefore, the study on the self-assembly behavior of diblock copolymers in $SCCO_2$ can yield useful information on the phase behavior of these systems, which could be used to control the size and morphology of the synthesized product particles.

The phase behavior of block copolymers in $SCCO_2$ depends on the polymer concentration, the temperature, and more dramatically the system pressure, as the density of near-critical fluids and of SCFs is strongly dependent on the system pressure. Therefore, the micellar behavior of a block copolymer in SCFs could be more complex than that in normal solvents. Several reports on the phase behavior of block copolymers in $SCCO_2$ have appeared in the literature. The association behavior of semifluorinated diblock alkane $F(CF_2)_{10}$-$(CH_2)_{10}H$ and of perfluoroalkylpoly(ethylene oxide) diblock surfactant, $F(CF_2)_{6-10}(CH_2CH_2O)_{3-8}H$, was studied by means of small-angle X-ray scattering (SAXS).[6] The micellar behavior of 1,1-dihydroperfluorooctyl acrylate-*b*-styrene diblock copolymer (PFOA-*b*-PS) and of PFOA-*g*-poly(ethylene oxide) (PFOA-*g*-PEO) graft copolymer in $SCCO_2$ was studied using small-angle neutron scattering (SANS).[7,8] The micellar behavior of PFOA-*b*-PS in $SCCO_2$ was also studied by means of nuclear magnetic resonance (NMR).[9] Very recently, light scattering studies[10,11] on the aggregation behavior of a poly(1,1-dihydroperfluorooctyl acrylate-*b*-vinyl acetate) diblock copolymer (PFOA-*b*-PVAc) in $SCCO_2$ was reported. The solubilities of many polymers in $SCCO_2$, including PVAc, PFOA, and poly(dimethylsiloxane) (PDMS), as well as the specific intermolecular interactions of $SCCO_2$ with those polymers[8,12−15] have provided additional information which can help us to understand the micellar behavior of block copolymers in $SCCO_2$. In previous works, the $SCCO_2$ density was used to represent its solvent strength.[7,14] It was concluded that the solvation of polymers in $SCCO_2$ could be related linearly to the solvent density.[14] Although the phase behavior of block copolymers in $SCCO_2$ changes significantly with the $SCCO_2$ density, density is not the only factor determining the phase behavior, because the same density value can be obtained using many different combinations of temperature and pressure values. In the present work,

* To whom correspondence should be addressed.

10.1021/ma980952d CCC: $18.00
Published on Web 08/19/1999

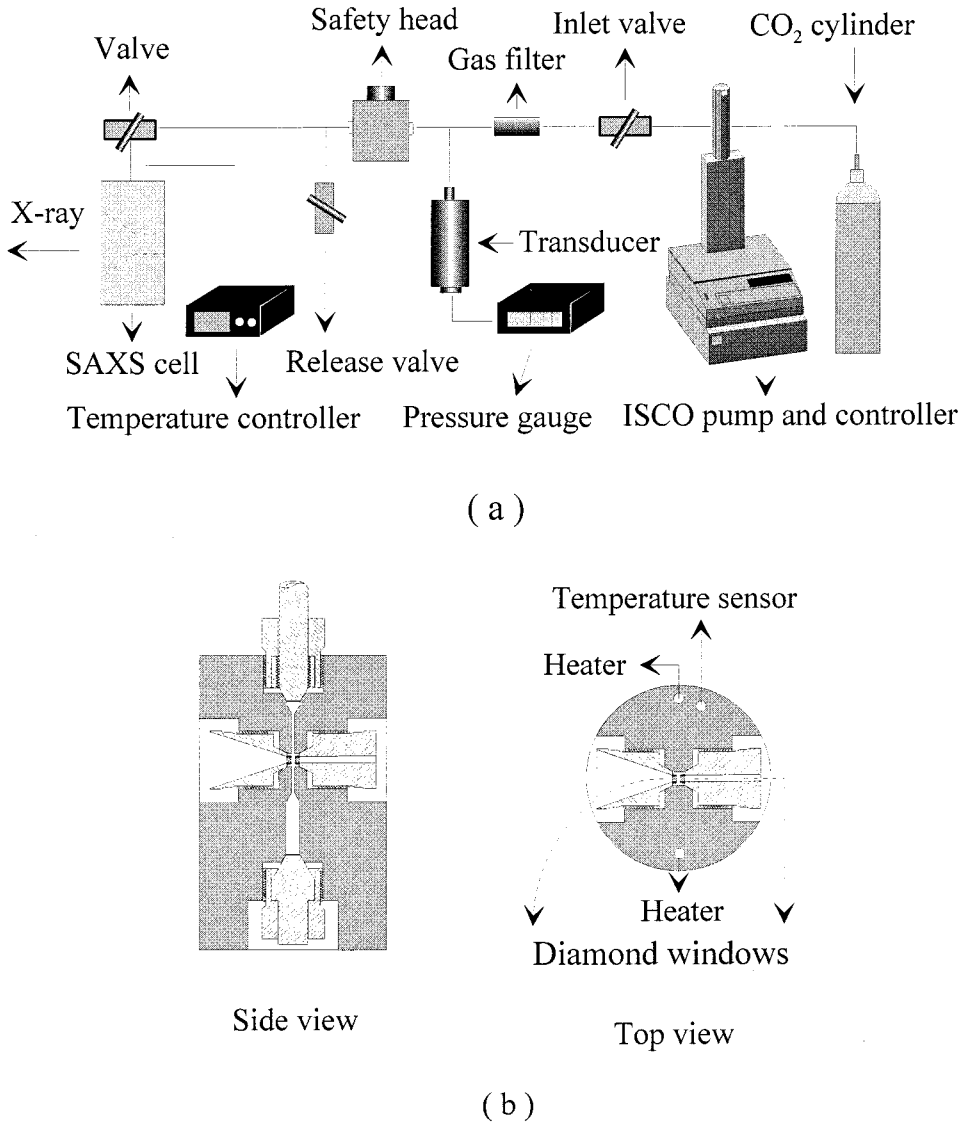

Figure 1. Schematic diagrams of the high-pressure apparatus for SAXS experiment: (a) overall diagram of the apparatus; (b) the cell design.

the phase behavior of poly(1,1-dihydroperfluorooctyl acrylate-*b*-vinyl acetate) diblock copolymer (PFOA-*b*-PVAc) in a dilute solution was investigated by using small-angle X-ray scattering (SAXS) for the following two processes: an isothermal process with changes in pressure and a cooling process at a constant pressure. The two independent processes (an isothermal process at different pressures and an isobaric process at different temperatures) can reveal the changes in the phase behavior of the block copolymer in $SCCO_2$ at constant $SCCO_2$ density. An isothermal experiment at 65 °C was conducted over a wide pressure range from 90 to 500 bar. An investigation on a cooling process from 65 to 20 °C starting from a micellar phase was conducted at a constant pressure of 243 bar. At a constant temperature, the aggregation behavior of the copolymer changed dramatically with pressure, while at a constant pressure, a strong dependence of the phase behavior on temperature was also observed. At a given $SCCO_2$ density, the phase behavior of the solution could be very different, including the species present and the micellar size; i.e., the phase behavior of a polymer in $SCCO_2$ should be considered as a function of two independent variables, e.g., pressure and temperature. It should also be noted that the phase behavior of polymers in $SCCO_2$ could be very sensitive to the system pressure at low pressures, as the solvent density $SCCO_2$ has a steep gradient with the pressure change, e.g., below 200 bar at 65 °C. The results obtained at 65 °C and at low pressures show that the PFOA-*b*-PVAc copolymer was first dissolved to form a soluble solution with increasing pressure and then started to form large aggregates with ordered internal domains when the pressure was further increased. With the pressure increased to about 240 bar, micelles were formed. The micelles could be broken up to become unimers again at about 450 bar. The self-assembly behavior of the copolymer solution could be related to the solubility of both blocks in $SCCO_2$.

Experimental Section

Sample. The PFOA-*b*-PVAc diblock copolymer was synthesized using the iniferter polymerization technique by first polymerizing the PVAc block.[16] The molecular weight of PVAc block was determined by GPC, and that of the PFOA block was determined by ^1H NMR. The molecular weights of PFOA and PVAc blocks are 43.1K and 10.3K, respectively.

High-Pressure Apparatus for Small-Angle X-ray Scattering. Figure 1a shows a schematic diagram of the high-pressure SAXS apparatus. A 100DX syringe pump with a temperature-controlled jacket, manufactured by ISCO Inc.,

was used to generate high pressures up to 10 000 psi. The carbon dioxide gas used was of supercritical fluid grade (SCF) CO_2 from the Scott Specialty Gases. The transducer (TH-1/INFS-0001-DC1 model), manufactured by Omegadyne Inc., was used together with a gauge for pressure reading. Figure 1b shows the details of the SAXS cell design. The cell was machined with 316 stainless steel. Diamond with a thickness of 1 mm was used for cell windows, and the window opening was 3 mm in diameter. The internal distance between the two diamond windows was about 3 mm. A Teflon-coated magnetic stirring bar could be placed in the bottom of the cell. Two heaters with a total power of 130 W were used to heat the high-pressure cell. The temperature inside the cell could be controlled to ±0.2 °C with an Omega temperature controller (model CN-76000). The high-pressure cell was first cleaned with acetone and then dust-freed by flowing filtered supercritical CO_2 through the manifold and the cell chamber. Finally, the whole system was pressurized and heated to the supercritical state, typically 200 bar and 40 °C. The pressure was released after the supercritical CO_2 had been kept for about 10 min in order to flush out possible impurities in the system. The procedure was repeated a few times before starting the experiment. After a polymer sample was introduced into the cell, the cell was first heated to the desired temperature (e.g., 65 °C) for an hour in order to ascertain that a equilibrium temperature was reached. Then the system was slowly pressurized, especially when the pressure was very close to a desired pressure, as the cool CO_2 would decrease the cell temperature. For our system, the experiment was done typically with a pressure precision ±0.4 bar. The experimental procedures for isothermal and isobaric processes were described as follows. For an isothermal process, the data were first collected at a fixed pressure, and then the pressure was increased to another value for data collection at the same temperature. For an isobaric process, the data were collected at given pressure and temperature, and then the temperature was decreased to the next desired temperature, while the pressure was maintained at a constant value by further introduction of CO_2 into the cell chamber.

Synchrotron Small-Angle X-ray Scattering (SAXS). The scattering experiments were performed at the SUNY X3-A2 beamline of the National Synchrotron Light Source (NSLS), Brookhaven National Laboratory (BNL). The X-ray wavelength used was 0.1283 nm. A pinhole collimation system was utilized with a sample-to-detector distance of 900 mm. Fuji imaging plates were used to collect the scattering data with exposure times of 3−5 min per frame, depending on the scattering power of the solution under the experimental conditions employed. The measured average radius gyration of the micelles and of the unimers in a dilute solution based on the data collected with an imaging plate was compared with the data collected with a one-dimensional Braun linear position-sensitive detector. The same values were obtained for both cases. The disadvantage of using the imaging plate is that the intensity collected can vary from one imaging plate to another depending on experimental conditions. Thus, it becomes more difficult to retrieve the data for the excess scattered intensity. However, the use of the two-dimensional imaging plate made the data collection much more efficient than a one-dimensional detector. Furthermore, it was easier for us to subtract the background scattering pattern from the diamond window. On the other hand, as the experiment was performed at high temperatures (65 °C), it was only prudent to reduce the experimental time period in order to avoid a possible loss of acetate units (lost as acetic acid vapor) in the PVAc block. The SAXS data at 243 bar were obtained by gradually pressurizing the system from 90 to ∼243 bar and took a total annealing time of about 16 h over a range of different pressures. This data set was compared with the results from a fresh sample by directly pressurizing the system to 243 bar. The radius gyration of micelles determined from the two data sets showed a perceptible difference of about 7%, suggesting that within our SAXS experiment time period the sample could have undergone a slight degradation, even though the 7% variable was within our experimental error limits. The scattering profiles were corrected for sample absorption, background, and incident X-ray intensity fluctuations.

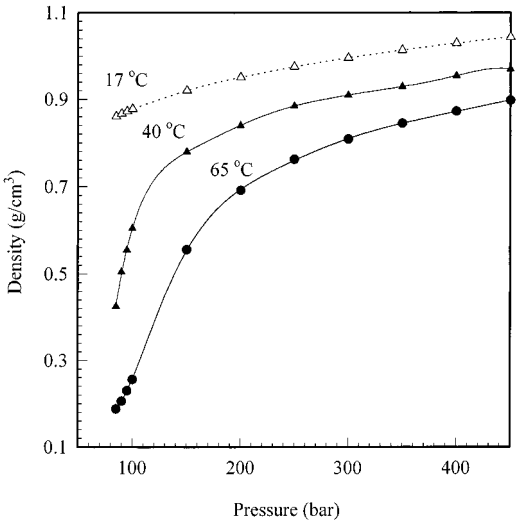

Figure 2. Density of $SCCO_2$ versus system pressure at different temperatures. (The data at 17 °C was from ref 18, and the data at 40 and 65 °C were interpolated from the data in ref 18.)

High-Pressure Laser Light Scattering (LLS). We have recently constructed a new high-pressure fiber-optic LLS spectrometer with gradient index of refraction microlenses as cell windows.[17] The experimental details for the LLS spectrometer have been described elsewhere.[10] Only a brief description is presented here. A Spectra-Physics model 165 argon ion laser operated at 488 nm was used as the light source. The PFOA-*b*-PVAC diblock copolymer was dust-freed as follows. First, the copolymer was dissolved in α,α,α-trifluorotoluene at 2×10^{-3} g/mL and then filtered carefully into a dust-free bottle by using 0.2 μm Millipore filters. The filtered solution was evaporated and vacuum-dried at 45 °C for 1 week. The high-pressure cell was dust-freed by flowing filtered supercritical CO_2 through the sample chamber for about 1 h before use. The clarified sample was added into the high-pressure cell from the exit window channel. Light scattering measurements were started after the solution had been stirred for 1−10 h and further equilibrated for 5−10 h, both depending on the working pressure and temperature. As the annealing time at 65 °C for light scattering experiments was appreciably longer than that for SAXS experiments, sample degradation could become a nonnegligible effect. Experiments were typically performed with a pressure and temperature precision of ±0.5 bar and ±0.2 °C, respectively. The light scattering data were collected at a scattering angle of 33.6°. Photon correlation measurements were carried out by using a Brookhaven Instruments digital correlator (BI9000).

Results and Discussion

Dissolution of Copolymer and Its Solution at Low Pressures (180 bar). The critical conditions for $SCCO_2$ are $T_c = 31.1$ °C and $P_c = 73.8$ bar. Figure 2 shows plots of $SCCO_2$ density versus the system pressure at different fixed temperatures.[18] It can be seen that the $SCCO_2$ density changes dramatically with pressure in the temperature range 40−60 °C and at pressures below ∼200 bar. The density increases from 0.2 to 0.68 g/cm^3 when the pressure is increased from 90 to 200 bar. As the $SCCO_2$ density is an important key factor governing its solvent quality and the density gradient versus pressure is very large within the pressure range from 90 to 200 bar, our experiments were performed at different fixed pressures with pressure changes down to 10 or 20 bar intervals, to avoid missing any specific "phase" change, such as aggrega-

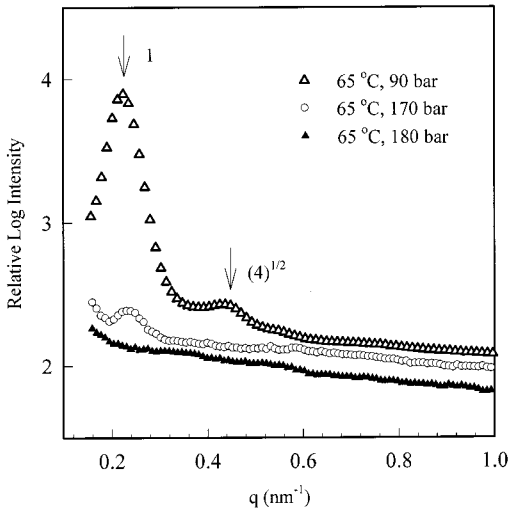

Figure 3. SAXS curves for the dissolution process of PFOA-*b*-PVAc block copolymer in 2 w/v % dilute solution. (CO_2 background has not been subtracted.)

tion, micelle formation, etc., within this pressure range. The experiment was started at a pressure of 90 bar for the dilute solution (2 w/v %) of PFOA-*b*-PVAc copolymer in $SCCO_2$. The copolymer sample was placed in the X-ray beam path in the high-pressure cell in order to probe the dissolution behavior of the PFOA-*b*-PVAc copolymer. The sample was first kept at 90 bar and 65 °C, a supercritical state for CO_2 but not too far from the critical point, for about 10 h before the first scattering image was collected. The SAXS scattering curve at 90 bar and 65 °C is shown in Figure 3. The strong SAXS scattering peak seen at $q_1 \sim 0.22$ nm^{-1} indicates that the sample under this condition was not soluble and still remained as a bulk sample with a phase-separated structure. The scattering curve showed the same characteristics as that of the bulk copolymer sample (not shown in Figure 3). As the molecular weight of the PVAc block is only about one-fifth of the PFOA block, the PVAc block is supposed to form a dispersed spherical domain in a PFOA matrix. A higher-order scattering peak is seen in Figure 3 at $q_2 \sim 0.44$ nm^{-1} with a ratio of q_1:q_2 to be 1:2, relative to the main scattering peak. It is suggested that a cubic PVAc domain packing has been formed in the PFOA matrix.

The sample was then kept at 110, 130, 150, 170, 180, and 190 bar for 1.5 h each before collecting the corresponding scattering data at these pressures. The scattered intensity of the main peak decreased with increasing pressure, as shown in Figure 3 for the scattering curve at 170 bar. This decrease in the scattered intensity was mainly caused by the dissolution of the copolymer; i.e., the higher the pressure, the more sample was dissolved in the solution. The above SAXS results are very similar to the NMR results obtained very recently on the PFOA homopolymer and the PFOA-*b*-PS diblock copolymer,[9] where a similar experiment was conducted at 65 °C. It was concluded from the NMR study that, in the above pressure range, the solubility of PFOA homopolymer in $SCCO_2$ kept increasing with increasing pressure and that both the homopolymer and the copolymer became soluble in $SCCO_2$ at about 220 bar. In our experiment, the scattering peaks disappeared when the pressure was increased to 180 bar, suggesting that the 2 w/v % copolymer became soluble in $SCCO_2$ at this pressure. As the molecular weight of the PFOA homopolymer used in the NMR study was 3 times larger than the PFOA block of the copolymer used in this work, the lower molecular weight PFOA block in our copolymer should become soluble at a lower pressure. The solubility of PVAc homopolymers in supercritical CO_2 was recently studied by Rindfleisch[12] et al. and by Kazarian[13] et al. The cloud-point data[12] showed that it took about 700 bar to dissolve PVAc in supercritical CO_2 at 65 °C. However, the molecular weight of the PVAC used in that work was about 12 times larger than the molecular weight of the PVAc block in our block copolymer; i.e., our block copolymer had a lower molecular weight PVAc block which should be soluble at a much lower pressure. Furthermore, the PVAc block in our copolymer had only one-fifth of the molecular weight of the copolymer. Therefore, the copolymer could be soluble at 180 bar in terms of the solubility of both PFOA and PVAc blocks in supercritical CO_2 as discussed above.

The diffusion coefficients are 10−100 times higher in supercritical fluids than in a normal liquid. Thus, it should take less time for the polymers to dissolve in SCFs. Our study on the dissolution behavior of a 2 w/v % copolymer in $SCCO_2$ by directly increasing the pressure to 180 bar showed that the scattering data collected after a 20 min equilibration time became comparable to the scattering curve in Figure 3 at 180 bar (denoted by solid triangles). Therefore, the 1.5 h equilibration time before data collection was considered to be sufficient. The density difference between the $SCCO_2$ ($\sim$0.65 g/cm^3 at 180 bar) and the copolymer ($\sim$1.17 for solid PVAc[19] and $\sim$1.63 for solid PFOA[9]) is very large, implying a large electron density difference and therefore a relatively strong excess scattered intensity. The average radius gyration of the copolymer unimer coils in $SCCO_2$ at 180 bar can be calculated by using the Guinier plot.[20]

$$I(q) \propto \exp[(-R_g^2/3)q^2] \quad (1)$$

where $I(q)$ is the excess scattered intensity, q is the scattering wave vector, and R_g is the average radius of gyration of the unimer coils, given by $R_g = (3/5)^{1/2}R$ for a sphere with radius R. The R_g can be calculated from the initial slope at low q values in a plot of $\ln(I(q))$ versus q^2. The scattering data of a dilute copolymer solution in $SCCO_2$ at 180 bar lies in a straight line up to $q^2 = 2$ nm^{-2} (shown to 0.3 nm^{-1} in Figure 4), suggesting that the solution is relatively homogeneous with R_g(180 bar) $= 3.4 \pm 0.3$ nm.

On the basis of a core−shell model where the PVAc block forms the core with a bulk PVAc density and the PFOA block forms a less compact shell containing the $SCCO_2$, the scattering behavior of the unimer could be simulated. According to the molecular weight of the PVAc block and its bulk density (1.17 g/cm^3), the calculated radius of the PVAc core was 1.52 nm. A PFOA homopolymer with a molecular weight of 43.1K should have a R_g value of 2.1 nm in $SCCO_2$, as determined from the scaling equation $(R_g^2/M_w)^{0.5} = 0.010$ nm.[14] By assuming that the PFOA homopolymer coil had a spherical morphology and a uniform density, the radius R of a spherical coil of the homopolymer and hence the coil volume could be estimated on the basis of its R_g value and the relation $R = (5/3)R_g$. On the basis of the PVAc core volume calculated from the estimated core radius and the assumption that the PFOA shell of the copolymer unimer took up the same volume in

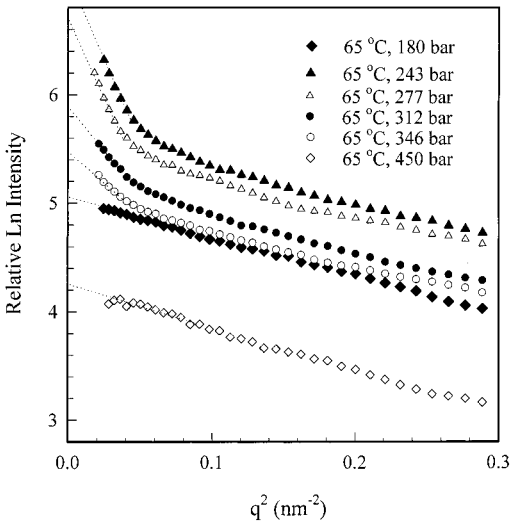

Figure 4. Guinier plot of SAXS data of 2 w/v % dilute solution in supercritical CO_2 at pressure 180, 243, 277, 312, 346, and 450 bar.

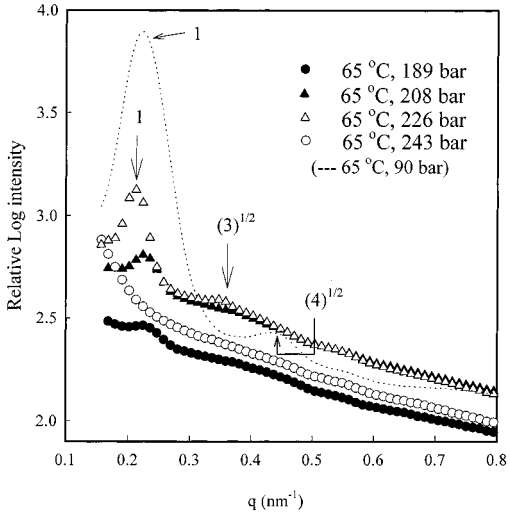

Figure 5. SAXS curves on the formation of large aggregates with internal-domain-packing structures in 2 w/v % dilute solution. (CO_2 background has not been subtracted.)

$SCCO_2$ as the PFOA homopolymer of the same molecular weight (43.1K), the total volume of the block copolymer unimer could be calculated. Thus, the radius of the unimer (including the core and the shell) could be estimated to be about 3.60 nm. From the above parameters, the R_g of the unimer could be computed as follows.

$$(M/(6.022 \times 10^{23}))R_g^2 = \int_0^{1.52} 4\pi\rho_{core} r^4 \, dr + \int_{1.52}^{3.60} 4\pi\rho_{shell} r^4 \, dr \quad (2)$$

where M is the copolymer molecular weight, ρ_{core} is the PVAc density in the core region, and ρ_{shell} is the PFOA density in the shell region. The calculated R_g value was about 2.7 nm. A unimer core−shell model having PVAc as the core and PFOA as the shell could also be used to compute a R_g value for the unimer. For a monodisperse system, the total scattering $I(q) \propto nP(q)S(q)$, where n, $P(q)$, and $S(q)$ are the number density of particles, the particle form factor, and the structure factor, respectively. When such a monodisperse system is sufficiently dilute, the scattering from interactions among the particles are negligible ($S(q) = 1$), and the scattered intensity $I(q) \propto nP(q)$. For a core−shell model, $P(q)$[21] can be written as follows

$$P(q) = [V_{core}(\rho_{core} - \rho_{shell}) f(qR_{core}) + V_{total}(\rho_{shell} - \rho_{solvent}) f(qR_{shell})]^2 \quad (3)$$

where R is the radius, ρ is the electron density, the function $f(x) = 3(\sin x - x \cos x)/x^3$, the core volume $V_{core} = (4/3)\pi R_{core}^3$, and the overall volume $V_{total} = (4/3)\pi R_{shell}^3$. By using the Guinier plot, R_g can be determined. The simulation was done for the system at 180 bar and 65 °C where the ρ_{core}, ρ_{shell}, and $\rho_{solvent}$ were taken to be 377, 266, and 196 e^-/nm^3, as well as at 450 bar and 65 °C where the ρ_{core}, ρ_{shell}, and $\rho_{solvent}$ were 377, 321, and 270 e^-/nm^3. A similar R_g value of 2.8 nm was obtained under this simulation condition. In fact, if the PVAc did form a core, this core was expected to be partially swollen by $SCCO_2$. Thus, the unimer R_g should be expected to be a little larger than the estimated value of 2.8 nm. Thus, the measured R_g value of 3.4 ± 0.3 nm was reasonable, suggesting that the copolymer in the soluble solution at 180 bar existed mainly as unimers.

Copolymer Aggregates with Internal-Domain-Packing Structure. The density of near-critical fluids and of supercritical fluids is strongly dependent on the pressure of the system, especially in the near-critical pressure range, e.g., when the pressure is increased from 90 to 180 bar at 65 °C, the density of $SCCO_2$ is increased from 0.22 to 0.65 g/cm^3, while with a further increase in pressure to 450 bar, the density only shows an increase to 0.90 g/cm^3. The strong dependence of $SCCO_2$ density on pressure, and hence a strong dependence of the solvent quality on pressure, is an advantage to using $SCCO_2$ as a solvent. The results in the previous section showed that the PFOA-*b*-PVAc copolymer in a dilute solution of $SCCO_2$ at 180 bar existed as unimers. With further increases in pressure, we continued to use an annealing time of 1.5 h at each pressure. Figure 5 shows that when the pressure was increased to 189 bar, a scattering peak at $q \sim 0.23$ nm^{-1} started to appear. Furthermore, the peak intensity increased with increasing pressure up to 226 bar, where the phase structure was well-developed. As a result, a higher-order scattering peak could be observed at $q \sim 0.35$ nm^{-1} with the main scattering peak at $q \sim 0.23$ nm^{-1} (corresponding to a d spacing of 27 nm). The sharp main peak suggests the presence of large aggregates with internal-domain-packing structures. The experiment could be repeated and thereby confirmed the above observation of the scattering pattern.

A dynamic laser light scattering study was also conducted to explore the self-assembly behavior of the copolymers in the same solution. Two selected figures are shown in Figures 6 and 7. The first peak with a hydrodynamic radius (R_h) of about 3 nm in Figure 6 could be attributed to the scattering from unimers, while the second peak with a hydrodynamic radius of about 300 nm at the peak maximum was due to the large aggregates. The scattered intensity ratio produced by the large aggregates and the unimers could be determined from the ratio of two peak areas, and this ratio at 225 bar was approximately equal to 1:1, as seen in Figure 6, implying that the weight fraction of the copolymer forming the large aggregates was very small and consisted of less than 1% of the copolymer solute.

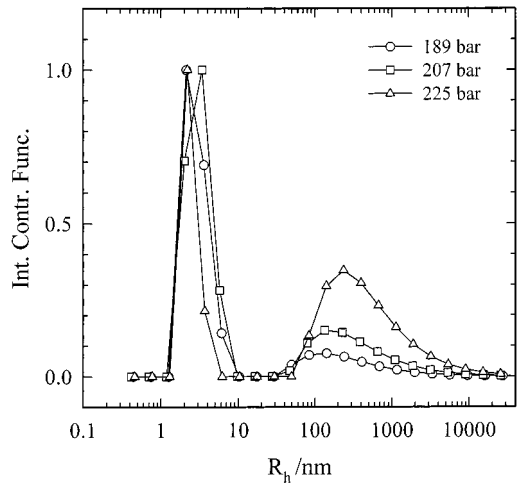

Figure 6. Laser light scattering measurements of 2 w/v % dilute solution in supercritical CO_2 at 65 °C for pressures ranging from 189 to 225 bar.

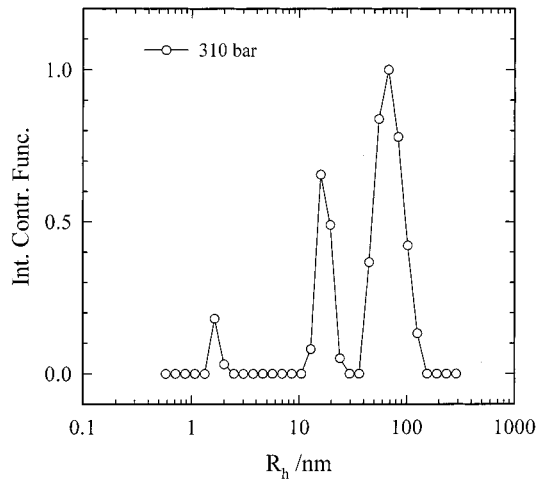

Figure 7. Laser light scattering measurements of 2 w/v % dilute solution in supercritical CO_2 at 65 °C and 310 bar.

The large aggregates could produce much stronger scattered intensity than the smaller ones. Large aggregates were also observed at other pressures but with a much smaller average hydrodynamic radius (70−100 nm), as shown, for example, in Figure 7 at 310 bar. No scattering peaks were observed from the SAXS study for the aggregates with $R_h < 100$ nm. However, the large aggregates formed at pressures from 189 to 225 bar could be much larger than those formed at other pressures. In Figure 6, the R_h values for the large aggregates at 225 bar ranged from 100 to 1500 nm. On the basis of both SAXS and light scattering results, it is quite clear that a very small portion of the copolymer in the solution at pressures from 189 to 226 bar formed large aggregates with internal-domain-packing structures.

The SAXS scattering pattern at 226 bar (Figure 5), including the main peak position, appears to be very similar to the scattering pattern at 90 bar, as shown in Figure 3, which represents the bulk structure of the copolymer before its dissolution. However, the two scattering curves at 90 and 226 bar show substantial differences in the peak position, the peak intensity, and the peak width. The peak position ratio q_1:q_2 for the curve obtained at 90 bar was 1:2, while this ratio was $1:(3)^{1/2}$ for the curve obtained at 226 bar. The PVAc domains at 226 bar could not have the lamellar morphology, in terms of the peak position ratio q_1:q_2 = $1:(3)^{1/2}$; presumably, they could still have a spherical morphology with a cubic packing structure. The continuous phase in the large aggregates should consist of the PFOA block and $SCCO_2$. The density of $SCCO_2$ at 189 and 226 bar is ~0.67 and 0.73 g/cm^3, respectively. An increase in the $SCCO_2$ density with increasing pressure would result in a decrease in the scattered intensity with increasing pressure. However, Figure 5 shows that when the pressure was increased from 189 to 226 bar, the overall scattered intensity increased, instead of decreased. The same intensity dependence on pressure was also observed from laser light scattering experiments. Figure 6 shows the peak due to the large aggregates was very weak at 189 bar, while a broader and larger peak was observed when the pressure was increased to 225 bar. The increase in the intensity of the LLS peak corresponding to the large aggregates (Figure 6) indicated that the weight fraction of the large aggregates in the solution increased with increasing pressure over the pressure range from 189 to 226 bar.

When the pressure was increased to 226 bar, the main SAXS peak was shifted to a lower q range. In addition, a higher-order scattering peak was also observed, as shown in Figure 5. The change in peak position and the presence of a higher-order scattering peak at 226 bar revealed the development of an ordered domain-packing structure. The SAXS intensity at 180 bar or higher was not comparable with that at 90 bar. In the former case, the polymer had been dissolved to form a homogeneous solution while in the latter case the polymer had not been dissolved completely. However, the peak widths at half-maximum intensity in the above two cases were comparable. The full width at half-maximum intensity at 90 bar was about 0.11 nm^{-1} while it was only about 0.04 nm^{-1} at 226 bar, as shown in Figure 5. The much narrower peak width at 226 bar than that at 90 bar suggested a more regular internal-domain-packing structure in the aggregates for the solution at 226 than that in the bulk copolymer. The peak width can also be expressed in terms of the crystallite size. The smaller the crystals, the broader the diffraction reflections. The crystallite size L can be estimated from the Scherrer equation[22]

$$L = 0.94\lambda/(B(2\theta)\cos\theta) \qquad (4)$$

where λ, 2θ, and $B(2\theta)$ are the wavelength, the diffraction angle, and the full width in radians subtended by the half-maximum intensity width of the diffraction peak. The calculated L value for the main peak at 226 bar was 180 nm, which could be approximately interpreted as an average crystallite dimension. The L value (180 nm) which could be considered as the ordered domain-packing size was comparable to the average aggregate size (~300 nm) from laser light scattering experiments.

Pressure and Temperature Dependence of Micellar Behavior. When the pressure was further increased to 243 bar, the solution showed a scattering decay, instead of a strong scattering peak, as shown by the scattering profile at 226 bar in Figure 5. The disappearance of the scattering peak indicated the dissolution of the large aggregates and suggested micellar formation. A Guinier plot of the scattering data ($\ln(I(q))$ versus q^2) shows a straight line at very low q values within the pressure range from 243 to 346 bar.

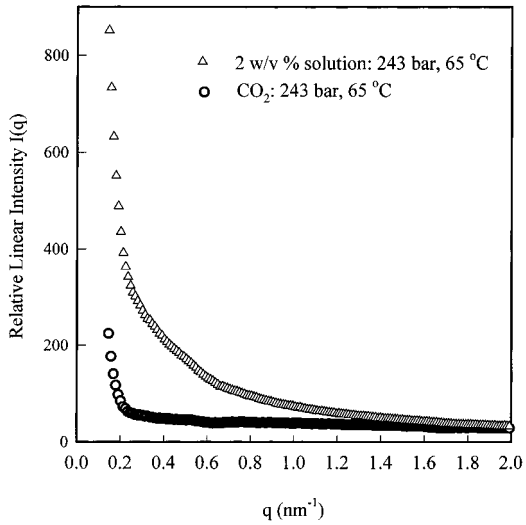

Figure 8. Relative linear scattered intensity of 2 w/v % dilute solution and pure supercritical CO_2 at 65 °C and 243 bar.

The slope of the straight line in the low q range was appreciably larger than that in the unimer state, as shown in Figure 4. The larger slope suggested the formation of micelles. A light scattering study[11] of this solution showed that a micellar solution with a small amount of unimers was formed at about 243 bar without the presence of any large aggregates. Therefore, when the pressure was increased from 226 to 243 bar, the large aggregates with dispersed PVAc microdomains were dissolved and micelles with a PVAc micellar core were formed. As the density of $SCCO_2$ within the above micellar pressure range was still appreciably smaller (~0.75 g/cm^3 at 243 bar) than that of the copolymer (~1.17 for solid PVAc[19] and ~1.63 for solid PFOA[9]), the net scattering from the copolymer micelles in the solution was considerably larger than the scattering background from the $SCCO_2$ and from the diamond windows, as shown for example in Figure 8 for the scattering profile at 243 bar. When the micelles were formed in solution, the scattered intensity could be much larger than that of the unimers in solution, as shown in Figure 4. The higher scattering was produced when the copolymer formed large aggregates. This is also seen in Figure 5 where the solution with large aggregates at 208 and 226 bar shows a much stronger scattered intensity than that of the solution with smaller micelles at 243 bar. The lower scattered intensity at 189 bar than that at 243 bar was presumably because only a small amount of the copolymer had formed the large aggregates at 189 bar.

Light scattering study[11] of the same solution did not show the presence of any large aggregates at 243 bar, but the large aggregates with a hydrodynamic radius ranging 70 to 100 nm were detected at some other pressures. These large aggregates did not produce the SAXS scattering peak, due to their smaller size. However, they could have a large contribution to the SAXS intensity in the low q range. Although the weight fraction of the large aggregates, estimated from the light scattering study, was only less than about 0.1% of the copolymer solute, it was necessary to know how the scattering contribution from the large aggregates would affect the SAXS data before the Guinier law could be used to determine the average R_g value of the micelles. The simulation results of the intensity $I(q)$ for a system with 1 wt % large spheres having a radius $R_g = 100$ nm and 99 wt % small spheres with a radius $R_g = 8$ nm are shown in Figure 9. The $P(q)$ was calculated with the following equation.

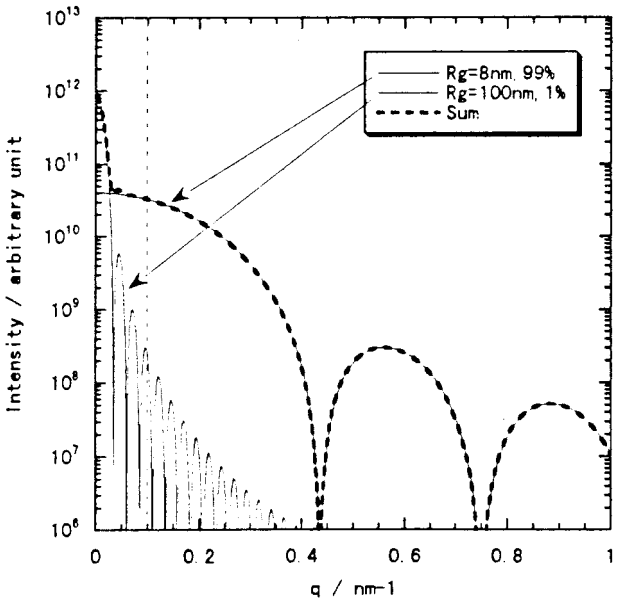

Figure 9. Simulation of scattering for a system with 99 wt % of spheres having a R_g value of 8 nm and 1 wt % of spheres having a R_g value of 100 nm. (The dashed line simulates the presence of a beam stop whereby the q range from 0 to 0.1 nm^{-1} could not be measured.)

$$P(q) = \{V\rho f(qR)\}^2 \tag{5}$$

where $V = (4/3)\pi R^3$, $f(x) = 3(\sin x - x \cos x)/x^3$, and ρ is the electron density difference between the particles and the surroundings (we assumed $\rho = 1$ in our simulation). It is seen from this figure that the contribution from the large aggregates is very small when compared with that from the small particles and is within the beam stop range for our experiment. Another simulation result indicates that the scattering from the large aggregates for the system with 5 wt % large aggregates ($R_g = 100$ nm) and 95 wt % small aggregates ($R_g = 8$ nm) still has almost no effect on the scattering curve in the range larger than $q = 0.1$ nm^{-1}. As the simulated system has 50 times more large aggregates by weight than that estimated from the light scattering experiment for the dilute solution, the scattering contribution in the small-angle scattering range from the large aggregates in solution could even be smaller. Therefore, the contribution from the large aggregates could be ignored in our SAXS data analysis because of the limited q range used in our SAXS measurements. In the micellar solution, the scattering from the unimers can also affect the scattered intensity. A light scattering study of the same solution was also conducted.[11] In comparing the q range of the light scattering experiment with that of the SAXS experiment, the q values for the former could be approximately considered as near zero, since the 488 nm wavelength used for the light scattering experiment was much larger than that (0.1283 nm) for the X-ray experiment. Therefore, the intensity ratio of the micelle to the unimer, obtained from our light scattering experiments, could be used as the approximate intensity ratio of the micelle to the unimer for our SAXS data in order to subtract the intensity contribution from the unimers. This information trans-

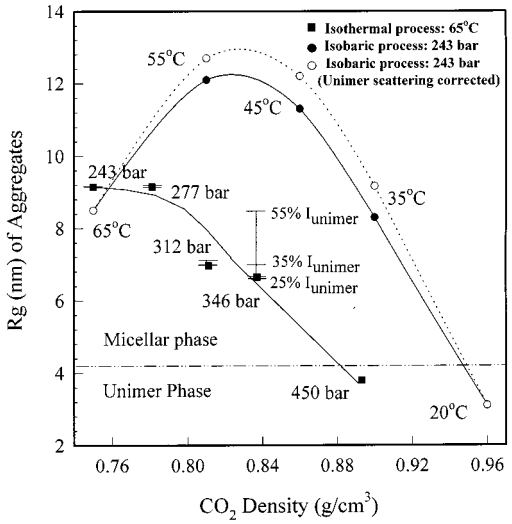

Figure 10. Average R_g of micelles/unimers versus $SCCO_2$ density for isothermal and isobaric processes. (The subtraction of the intensity contribution from unimers was based on the intensity ratio of micelle to unimer, obtained from our laser light scattering experiments.)

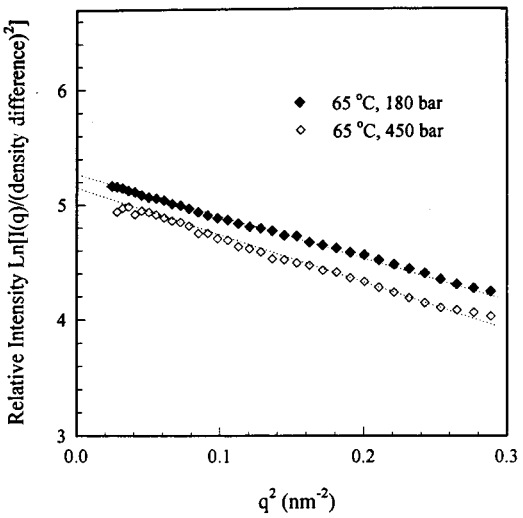

Figure 11. Guinier plot of SAXS data at 65 °C and 180 or 450 bar after the correction of SCCO2 density difference.

fer is acceptable provided that the refractive index difference is comparable to the electron density difference.

On the basis of the Guinier plot[20] but without a correction for the scattered intensity due to the unimers, the calculated average radius of gyration value for the micelles at 243 and 277 bar was 9.15 nm. When the pressure was further increased to 312 and 346 bar, the R_g value decreased to 6.97 and 6.65 nm, respectively, as shown in Figure 10. Figure 4 also shows that the Guinier plots for $q > 0.3$ nm^{-1}, i.e., $q^2 > 0.09$ nm^{-2}, are almost paralell. The scattering within this q range came mainly from unimers. The similarity of the plots within this q range suggsted that the unimers existed in the solution over the range of the pressures studied as shown in Figure 4 with little variation in the radius of gyration. In fact, the unimers were observed over same the pressures range from the light scattering study for this solution.[11] The light scattering study of an isothermal process at 65 °C showed that for pressures ranging from 243 to 310 bar the scattered intensity ratio of micelles to unimers increased with increasing pressure, but the intensity contribution from the unimers was less than 12% of the total intensity, as shown for example at 310 bar in Figure 7. Figure 10 shows that the scattering contribution from the unimers at pressures from 243 to 310 bar does not have an appreciable effect on the determination of micellar size by using the Guinier plot. The light scattering study showed that at 346 bar the intensity ratio of micelles to unimers was about 45:55, indicating an appreciable amount of unimers in the solution. Thus, a straightforward R_g calculation for the micelles at this pressure could contain an appreciable error. As the sample annealing time for light scattering experiments was appreciably longer than that for the SAXS experiments, the sample degradation in the light scattering experiments might not be negligible; i.e., the intensity contribution from unimers for our SAXS data could be smaller than that determined from the light scattering experiment. The intensity contribution from the unimers at 346 bar was probably of the order of 35%. In Figure 10, the error bars were shown for the R_g value at 346 bar by assuming that the intensity contribution from unimers was 25, 35, and 55%.

Decrease in the R_g value with increasing pressure could imply that the $SCCO_2$ became a better solvent for the copolymer at higher pressures. When the pressure was further increased to 450 bar, the scattering data in a plot of ln $I(q)$ versus q^2 lies on a straight line, as shown in Figure 4, suggesting that the copolymer again existed as unimers. When compared with the scattered intensity from micelles, it is seen in Figure 4 that the scattered intensity from unimers at 450 bar is much lower. The calculation based on the Guinier plot showed that the average radius of gyration of the unimers was 3.8 ± 0.3 nm. For the unimer state at 180 bar and that at 450 bar, as shown in Figure 4, the scattered intensity at the lower pressure was stronger than that at the higher pressure. The difference in the scattered intensity could be attributed to the large difference in the $SCCO_2$ density at the two pressures. The $SCCO_2$ density at 180 and 450 bar are 0.64 and 0.89 g/cm^3, respectively. Therefore, the density difference between the unimer segments and the $SCCO_2$ at 450 bar is appreciably smaller than that at 180 bar, resulting in a remarkably lower scattered intensity of the unimers at 450 bar. In Figure 11, the scattering curves of the unimer at 180 and 450 bar were approximately corrected for the density difference between the copolymer and the solvent at the two different pressures. After the correction, the scattered intensity of the unimers at 450 bar was fairly close to that at 180 bar. The average R_g value of the unimers at 180 bar was 3.4 ± 0.3 nm, while it was 3.8 ± 0.3 nm at 450 bar, probably suggesting that the $SCCO_2$ at 450 bar could be a better solvent for the copolymer than the $SCCO_2$ at 180 bar. When the copolymer solution in $SCCO_2$ was maintained at 65 °C for more than 30 h, the copolymer degradation could be detected as the R_g of the unimer was decreased to about 1.7 nm. In the present work, the total annealing time of the solution at 65 °C was about 16 h. When the pressure was increased to 450 bar, the unimer R_g value became a little bit larger than that at 180 bar, suggesting negligible degradation for the copolymer in our SAXS experiment time period.

The temperature dependence of micellar behavior has also been studied in the present work. The experiment was started from 243 bar and 65 °C, where no any large

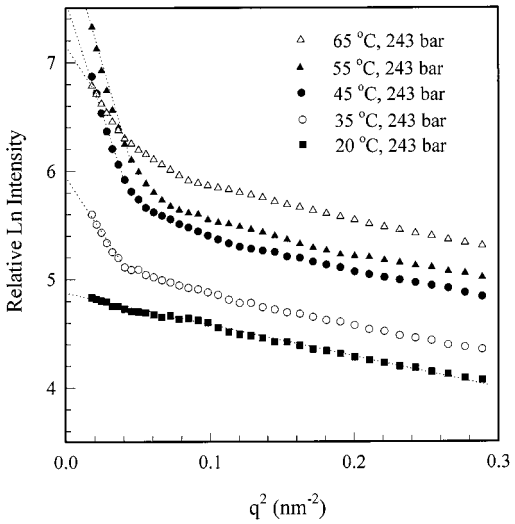

Figure 12. Guinier plot of SAXS data of 2 w/v % dilute solution in supercritical CO_2 during a cooling process at a constant pressure of 243 bar.

aggregates were present. Then a constant pressure of 243 bar was maintained, and the temperature of the solution was decreased from 65 to 20 °C. Figure 12 shows plots of ln $I(q)$ versus q^2 for the solution at temperatures 65, 55, 45, 35, and 20 °C. The light scattering study[11] showed that the intensity contribution fraction from unimers increased with decreasing temperature and that it was less than 10% above 40 °C. The light scattering experiment did not include an intensity ratio at 35 °C. On the basis of the intensity fraction of 9.3% for the unimer at 40 °C, an estimated intensity fraction of about 20% from unimers at 35 °C was used to correct the SAXS data. The average R_g values of the micelles at the above temperatures are also shown in Figure 10 before and after the correction of unimer scattering. In the temperature study, a fresh sample was used; the solution was directly pressurized to 243 bar and maintained for about 2 h before data collection. The obtained R_g value (8.6 nm) was slightly smaller than that (9.2 nm) obtained under the same conditions during the isothermal process with a total annealing time of about 9 h (Figure 10). The small discrepancy could be attributed to a slight degradation of the copolymer during the isothermal process. When the temperature was decreased from 65 to 55 °C, the average R_g value increased from 8.5 to 12.7 nm; with further decrease in the temperature to 45 °C and then to 35 °C, the R_g value decreased to 12.2 and 9.17 nm, respectively, as shown in Figure 10. Finally, when the CO_2 became a liquid at 20 °C, the copolymer existed mainly as unimers by showing a straight line in the Guinier plot (Figure 10). The calculated R_g value in the liquid CO_2 state was 3.1 ± 0.3 nm, which is smaller than the R_g values in the two unimer states in $SCCO_2$ at 180 and 450 bar and 65 °C. The larger R_g value for the unimers in $SCCO_2$ than that in liquid CO_2 suggested that the $SCCO_2$ could be a better solvent than the liquid CO_2. The isobaric experiments performed at different temperatures indicated that the $SCCO_2$ became a worse solvent for the copolymer at a higher temperature for the temperature range from 20 to 55 °C. When the temperature was increased from 55 to 65 °C, the $SCCO_2$ became a better solvent than it was at 55 °C. In Figure 10, the aggregate (or micellar) size is shown as a function of $SCCO_2$ density. The micellar size decreased with increasing $SCCO_2$ density for both the isothermal and the cooling process from 55 to 20 °C. The same dependence of micellar size on the $SCCO_2$ density was also reported in the literature.[7] The micellar size became appreciably smaller at 65 °C than that at 55 °C, as the $SCCO_2$ was a better solvent for the copolymer at 65 °C than that at 55 °C. The same conclusion was also reached from our laser light scattering study of the same solution.[11] A light scattering study of an isobaric process at 242 showed that unimer, micelle, and large aggregate species were present at 55 °C, while large aggregates disappeared at 65 °C, suggesting that the $SCCO_2$ was a better solvent at 65 °C than that at 55 °C. A light scattering study of an isobaric process at 225 bar showed that no micelles were formed at 65 and 75 °C, while the micelles were formed at 55 °C, and that when the temperature was further decreased, the micelle scattering decreased first and then disappeared. It should be noted that the micelle formation is a function of both pressure and temperature, instead of only a function of $SCCO_2$ density. At a given density, the micellar size in the isothermal process was appreciably smaller than that in the constant pressure process. On the other hand, at a density at about 0.9 g/cm^3, the copolymer formed micelles in $SCCO_2$ while it existed as unimers in liquid CO_2, as shown in Figure 10.

Conclusion

SAXS of a dilute solution (2 w/v %) of the PFOA-*b*-PVAc block copolymer in supercritical carbon dioxide shows that, in an isothermal process at 65 °C, a soluble solution of (mainly) unimer was obtained at a low pressure of 180 bar ($\rho \sim 0.65$ g/cm^3) with $R_g = 3.4 \pm 0.3$ nm and at a high pressure of 450 bar ($\rho \sim 0.90$ g/cm^3) with $R_g = 3.8 \pm 0.3$ nm. When the solution was cooled from 65 to 20 °C and at a constant pressure of 243 bar, a block copolymer solution of unimers was also observed at 20 °C with CO_2 in the liquid state. However, the average R_g (3.1 ± 0.3 nm) of the unimers is smaller than that in the $SCCO_2$ state (3.4 ± 0.3 to 3.8 ± 0.3 nm), suggesting that the $SCCO_2$ could be a better solvent than the liquid CO_2 for the copolymer.

In the isothermal process at 65 °C, large aggregates were observed at 190 bar *after* the polymer had been dissolved in solution as unimers at 180 bar. When the pressure was increased to 226 bar, an internal-domain-packing structure was formed inside the large aggregates with an average hydrodynamic radius of about 300 nm, even though the amount of large aggregates was very small when compared with the unimers/micelles as shown by dynamic light scattering analysis.

A micellar phase was observed at 243 bar and 65 °C, and the micellar behavior of the solution was studied by increasing the pressure at a constant temperature (65 °C) and by decreasing the temperature at a constant pressure (243 bar) from this state. The micellar size shows a similar dependence on the solution density at the above two processes. However, the dependence of the phase behavior on the density for the two processes could be very different, including the nature of the species and the micellar size. The differences for the two different processes indicate that the block copolymer solution behavior in $SCCO_2$ is governed by both pressure and temperature, instead of just the $SCCO_2$ density.

Acknowledgment. B.C. gratefully acknowledges the support of this work by the U.S. Department of

Energy (DE-FG02-86ER45237.015) and the SUNY X3 Beamline at the National Synchrotron Light Source, supported by the Division of Basic Energy Sciences of the U.S. Department of Energy (DE-FG02-86ER45231). He also thanks Prof. Joseph M. DeSimone, from the University of North Carolina at Chapel Hill, for providing the copolymer sample, and Dr. John L. Fulton, from Pacific Northwest Laboratory, for his help in the design of the high-pressure SAXS chamber.

References and Notes

(1) McHugh, M. A.; Krukonis, V. J. *Supercritical Critical Extraction*; Butterworths: Boston, 1996.
(2) *Chemical Engineering at Supercritical Fluid Conditions*; Paulaitis, M. E., Penninger, J. M. L., Gary, R. D., Davidson, R., Eds.; Ann Arbor Science Publisher: Ann Arbor, MI, 1984.
(3) DeSimone, J. M.; Guan, Z.; Elsbernd, C. S. *Science* **1992**, *257*, 945.
(4) Kapellen, K. K.; Mistele, C. D.; DeSimone, J. M. *Macromolecules* **1996**, *29*, 495.
(5) Canelas, D. A.; Betts, D. E.; DeSimone, J. M. *Macromolecules* **1996**, *29*, 2818.
(6) Fulton, J. L.; Pfund, D. M.; McClain, J. B.; Romack, T. J.; Maury, E. E.; Combes, J. R.; Samulski, E. T.; DeSimone, J. M.; Capel, M. *Langmuir* **1995**, *11*, 4241.
(7) McClain, J. B.; Betts, D. E.; Canelas, D. A.; Samulski, E. T.; DeSimone, J. M.; Londono, J. D.; Cochran, H. D.; Wignall, G. D.; Chillura-Martino, D.; Triolo, R. *Science* **1996**, *274*, 2049.
(8) Chillura-Martino, D.; Triolo, R.; McClain, J. B.; Combes, J. R.; Betts, D. E.; Canelas, D. A.; DeSimone, J. M.; Samulski, E. T.; Cochran, H. D.; Londono, J. D.; Wignall, G. D. *J. Mol. Struct.* **1996**, *383*, 3.
(9) Dardi, Alexander; Cain, J. B.; DeSimone, J. M.; Johnson, C. S., Jr.; Samulski, E. L. *Macromolecules* **1997**, *30*, 3593.
(10) Zhou, S.; Chu, B. *Macromolecules* **1998**, *31*, 5300.
(11) Zhou, S.; Chu, B. *Macromolecules* **1998**, *31*, 7746.
(12) Rindfleisch, F.; DiNoia, T. P.; McHugh, M. A. *J. Phys. Chem.* **1996**, *100*, 15581.
(13) Kazarian, S. G.; Vincent, M. F.; Bright, F. V.; Liotta, C. L.; Eckert, C. A. *J. Am. Chem. Soc.* **1996**, *118*, 1729.
(14) McClain, J. B.; Londono, D.; Combes, J. R.; Romack, T. J.; Canelas, D. A.; Betts, D. E.; Wignall, G. D.; Samulski, E. T.; Desimone. J. M. *J. Am. Chem. Soc.* **1996**, *118*, 917.
(15) Hoefling, T. A.; Enick, R. M.; Beckman, E. J. *J. Phys. Chem.* **1991**, *95*, 7127.
(16) Betts, D.; Johson, T.; Anderson, C.; DeSimone, J. M. *Polym. Prepr.* **1997**, *38* (1), 760.
(17) Zhou, S. Q.; Chu, B.; Dhadwal, H. S. *Rev. Sci. Instrum.* **1998**, *69*, 1955.
(18) Angus, S.; Armstrong, B.; de Reuck, K. M. *International Thermodynamic Tables of the Fluid State Carbon Dioxide;* Pergamon Press: London, UK, 1973.
(19) *Polymer Handbook*, 2nd ed.; Brandrup, J., Immergut, E. H., McDowell, W., Eds.; Wiley-Interscience Publication: New York, 1975.
(20) Guinier, A.; Fournet, G. *Small-Angle Scattering of X-rays*; John Wiley & Sons: London, 1955.
(21) Wu, G.; Chu, B.; Schneider, D. K. *J. Phys. Chem.* **1994**, *98*, 12018.
(22) Warren, B. E. *X-ray Diffraction*; Dover Publications: New York, 1990.

MA980952D